JNCI J Natl Cancer Inst (2015) 107(5): djv053

doi:10.1093/jnci/djv053
First published online March 12, 2015
Brief Communication

BRIEF COMMUNICATION

Whole-Exome Sequencing Identifies *MDH2* as a New Familial Paraganglioma Gene

Alberto Cascón*, Iñaki Comino-Méndez*, María Currás-Freixes, Aguirre A. de Cubas, Laura Contreras, Susan Richter, Mirko Peitzsch, Veronika Mancikova, Lucía Inglada-Pérez, Andrés Pérez-Barrios, María Calatayud, Sharona Azriel, Rosa Villar-Vicente, Javier Aller, Fernando Setién, Sebastian Moran, Juan F. Garcia, Ana Río-Machín, Rocío Letón, Álvaro Gómez-Graña, María Apellániz-Ruiz, Giovanna Roncador, Manel Esteller, Cristina Rodríguez-Antona, Jorgina Satrústegui, Graeme Eisenhofer, Miguel Urioste, Mercedes Robledo

Affiliations of authors: Hereditary Endocrine Cancer Group, Spanish National Cancer Research Centre, Madrid, Spain (AC, ICM, MCF, AAdC, VM, LIP, RL, AGG, MAR, CRA, MR); Centro de Investigación Biomédica en Red de Enfermedades Raras, Madrid, Spain (AC, LC, LIP, CRA, JS, MU, MR); Departamento de Biología Molecular, Centro de Biología Molecular Severo Ochoa UAM-CSIC, Universidad Autónoma de Madrid and Instituto de Investigación Sanitaria Fundación Jiménez Díaz, Madrid, Spain (LC, JS); Institute of Clinical Chemistry and Laboratory Medicine, University Hospital Carl Gustav Carus, Medical Faculty Carl Gustav Carus, Technische Universität Dresden, Dresden, Germany (SR, MP, GE); Departments of Pathology (APB) and Endocrinology and Nutrition Service (MC), Hospital 12 de Octubre, Madrid, Spain; Endocrinology Service, Hospital Infanta Sofía, San Sebastián de los Reyes, Spain (SA); Department of Endocrinology and Nutrition Service, Hospital de Fuenlabrada, Madrid, Spain (RVV); Endocrinology Service, Hospital Puerta de Hierro, Majadahonda, Madrid, Spain (JA); Cancer Epigenetics and Biology Program, Bellvitge Biomedical Research Institute, L'Hospitalet, Barcelona, Spain (FS, SM, ME); Department of Pathology, MD Anderson Cancer Center Madrid, Madrid, Spain (JFG); Molecular Cytogenetics Group (ARM), Monoclonal Antibodies Unit, Biotechnology Programme (GR), and Familial Cancer Clinical Unit (MU), Spanish National Cancer Research Centre, Madrid, Spain.
*Authors contributed equally to this work.

Correspondence to: Alberto Cascón, PhD, Hereditary Endocrine Cancer Group, Human Cancer Genetics Programme, Spanish National Cancer Research Centre, Melchor Fernández Almagro 3, 28029 Madrid, Spain (e-mail: acascon@cnio.es) or Mercedes Robledo, PhD, Hereditary Endocrine Cancer Group, Human Cancer Genetics Programme, Spanish National Cancer Research Centre, Melchor Fernández Almagro 3, 28029 Madrid, Spain (e-mail: mrobledo@cnio.es).

Abstract

Disruption of the Krebs cycle is a hallmark of cancer. IDH1 and IDH2 mutations are found in many neoplasms, and germline alterations in SDH genes and FH predispose to pheochromocytoma/paraganglioma and other cancers. We describe a paraganglioma family carrying a germline mutation in MDH2, which encodes a Krebs cycle enzyme. Whole-exome sequencing was applied to tumor DNA obtained from a man age 55 years diagnosed with multiple malignant paragangliomas. Data were analyzed with the two-sided Student's t and Mann-Whitney U tests with Bonferroni correction for multiple comparisons. Between six- and 14-fold lower levels of MDH2 expression were observed in MDH2-mutated tumors compared with control patients. Knockdown (KD) of MDH2 in HeLa cells by shRNA triggered the accumulation of both malate (mean ± SD: wild-type [WT] = 1 ± 0.18; KD = 2.24 ± 0.17, $P = .043$) and fumarate (WT = 1 ± 0.06; KD = 2.6 ± 0.25, $P = .033$), which was reversed by transient introduction of WT MDH2 cDNA. Segregation of the mutation with disease and absence of MDH2 in mutated tumors revealed MDH2 as a novel pheochromocytoma/paraganglioma susceptibility gene.

Pheochromocytomas and paragangliomas are tumors that mainly arise from the adrenal medulla and the sympathetic nervous system paraganglia, respectively. Since 1990, 11 major susceptibility genes have been identified: *NF1*, *RET*, *VHL*, *SDHA*, *SDHB*, *SDHC*, *SDHD*, *SDHAF2*, *TMEM127*, *MAX*, and *FH* (1). However, there are still some patients with clinical indicators

Received: April 17, 2014; **Revised:** September 11, 2014; **Accepted:** February 9, 2015

© The Author 2015. Published by Oxford University Press. All rights reserved. For Permissions, please e-mail: journals.permissions@oup.com.

Downloaded from https://academic.oup.com/jnci/article/107/5/djv053/891892 by guest on 25 August 2022

of hereditary disease (ie, family history, multiple tumors, and/or young age) that are not explained by mutations in these genes.

Whole-exome sequencing was applied to tumor DNA obtained from a man age 55 years who was diagnosed with multiple malignant paragangliomas. Details about patients, sequencing methods, reverse transcriptase and quantitative real-time polymerase chain reaction, western blot analyses, immunohistochemistry, gene expression, and enzymatic activity analyses, and cell culture are available in Supplementary Methods (available online). The Kolmogorov-Smirnov test was used to assess departure from the normal distribution. When a normal distribution could not be assumed, a two-sided exact Mann-Whitney U test was applied to test for differences. Otherwise a *t* test for independent samples was applied. Nominal two-sided *P* values less than .05 were considered statistically significant. Statistical analyses were performed using SPSS version 17 (SPSS Inc., Chicago, IL), R version 3.0.1 and Graphpad Instat version 3.05. The Instituto de Salud Carlos III (ISCIII) ethics committee approved the study, and the patients or their relatives provided written informed consent.

Five single nucleotide substitutions and 11 insertions or deletions (INDELs) passed the filtering process (Supplementary Table 1, available online). These included a heterozygous variant, c.429+1G>T, affecting a canonical donor splice site on exon 4 of *MDH2*, the gene that encodes the mitochondrial malate dehydrogenase enzyme involved in the Krebs cycle. After confirming the presence of the variant in the sequenced tumor and in peripheral blood lymphocytes from the patient, Sanger sequencing of the available primary tumors from the patient (n = 4) revealed loss of the *MDH2* wild-type allele in two tumors, indicating loss of heterozygosity (Figure 1A). Direct sequencing of the cDNA regions flanking the mutation demonstrated that c.429+1G>T gave rise to an altered transcript that incorporated 20 additional amino acids into the exon as well as to a premature stop codon. Because the stop codon is followed by more than 50 nucleotides, it was considered potentially involved in nonsense-mediated decay (Figure 1B) (2). MDH2 mRNA expression analysis revealed six- to 14-fold lower levels of MDH2 expression in the four tumors carrying the c.429+1G>T mutation, compared with control patients (Figure 1C). In addition, substantially lower levels of MDH2 protein were detected in the *MDH2*-related tumors compared with control patients (Figure 1D), suggesting that nonsense-mediated decay was occurring and confirming loss of expression of the wild-type allele in all mutated tumors. The *MDH2*-mutated tumor displayed statistically significantly lower MDH2 activity than that of control tumors (median [range] = 275.78 nmol/min/mg [181.69–882.43] vs 966.64 nmol/min/mg [221.07 - 3551.0]; *P* = .006) (Figure 1E), suggesting severe malate dehydrogenase deficiency. Krebs cycle metabolite analysis did not detect accumulation of malate in the *MDH2*-mutated tumor. However, a much higher fumarate:succinate ratio was observed in the *MDH2*-mutated tumor (mean of two measurements = 0.34) in comparison with succinate dehydrogenase (SDH) gene-mutated (mean ± SD = 0.01 ± 0.02; *P* = .044) and non-mutated (mean ± SD: 0.06 ± 0.10; *P* = .006) tumors (Supplementary Figure 1, available online), suggesting that fumarate could be accumulated in *MDH2*-mutated cells. Knockdown of MDH2 expression in HeLa cells by shRNA (Supplementary Figure 2, A-C, available online) triggered the accumulation of both malate (mean ± SD: wild-type [WT] = 1 ± 0.18 vs KD = 2.24 ± 0.17; *P* = .043) and fumarate (mean ± SD: WT = 1 ± 0.06 vs KD = 2.6 ± 0.25 [WT]; *P* = .033) which was reverted by transient introduction of wild-type MDH2 cDNA (Figure 1, F-H). Additional malate-utilizing enzymes (MDH1 and malic enzymes 1–3) could be responsible for the absence of malate accumulation in *MDH2*-mutated tumors. However, neither the observed MDH1 activity (Supplementary Table 2, available online) nor the expression of malic enzymes 1–3 (data not shown) in the *MDH2*-mutated tumors explain the absence of malate accumulation, suggesting that an unknown mechanism is accounting for this controversial result.

Several studies have demonstrated that the accumulation of succinate and fumarate, caused by SDH gene mutations and *FH* mutations, respectively, and the production of 2-hydroxyglutarate (2HG), associated with *IDH1* and *IDH2* alterations, lead to the enzymatic inhibition of multiple α-KG-dependent dioxygenases (3,4). This inhibition causes impaired histone demethylation and 5-mC hydroxylation (5-hmC) and, consequently, genome-wide histone and DNA methylation alterations. This in turn leads to a characteristic CpG island methylator phenotype (CIMP) (5) and provides a rationale for tumor development caused by Krebs cycle disruption. Expression profiling analysis based on genes that were hypermethylated and downregulated in SDH gene- and *FH*-mutated tumors and associated with the characteristic CIMP (5) revealed that the *MDH2*-mutated tumor and three apparently sporadic cases all clustered with SDH gene-mutated tumors, suggesting a similar CIMP (CIMP-like) profile (Figure 2A). Immunohistochemical evaluation of 5-hmC (Figure 2B) and trimethylation of histone H3 lysine 27 (H3K27me3) (Supplementary Figure 3A, available online) were also consistent with the *MDH2*-mutated tumor having a CIMP-like profile. In addition, classification by retinol binding protein 1 (*RBP1*) expression, which is an exclusive biomarker for *IDH* mutations in gliomas (6), segregated the *MDH2*- with the SDH-mutated tumors (Figure 2C; Supplementary Figure 3B, available online), providing further evidence that *MDH2* mutations are associated with a methylator phenotype. Finally, methylation analysis based on pyrosequencing of CpG sites in seven selected genes (including *RBP1*) (Supplementary Figure 3C, available online) demonstrated that the genome-wide downregulation observed for the *MDH2*-mutated tumors was because of CpG island methylation.

A genetic study of five asymptomatic relatives of the patient found that two of them carried the *MDH2* c.429+1G>T mutation. MDH2 mRNA and protein expression in blood cells were statistically significantly lower in the two carriers compared with control patients (median ± SD: 0.33 ± 0.07 [*P* = .0001] and 0.53 ± 0.05 [*P* = .0001] vs 1.08 ± 0.08, respectively), confirming that the splicing mutation has a deleterious effect (Supplementary Figure 4, available online). Subsequent clinical testing detected high levels of normetanephrine for one of the carriers (II-2), thus confirming the presence of the disease. Neither the three apparently sporadic cases with tumors that grouped within the CIMP-like cluster nor a selected series of cases with clinical features of a hereditary disease (Supplementary Table 3, available online) had alterations in the *MDH2* gene.

During the last 10 years, germline and acquired alterations affecting some of the enzymes involved in the Krebs cycle have been recognized as one of the hallmarks of cancer, and, more specifically, of pheochromocytoma/paraganglioma development. It is well known that germline mutations in the genes encoding the four structural subunits of the Krebs cycle enzyme SDH (7–10), or in the regulatory enzyme SDHAF2 (11), predispose to hereditary pheochromocytoma/paraganglioma. In addition, inactivating mutations in *FH* predispose to hereditary leiomyomatosis and renal cell cancer (HLRCC) (12) and have recently been identified in patients with pheochromocytoma/paraganglioma (5,13). Finally, *IDH1* and *IDH2* are frequently mutated in multiple types of human cancer, including one paraganglioma (14). In the present study, we have demonstrated the deleterious

Downloaded from https://academic.oup.com/jnci/article/107/5/djv053/891892 by guest on 25 August 2022

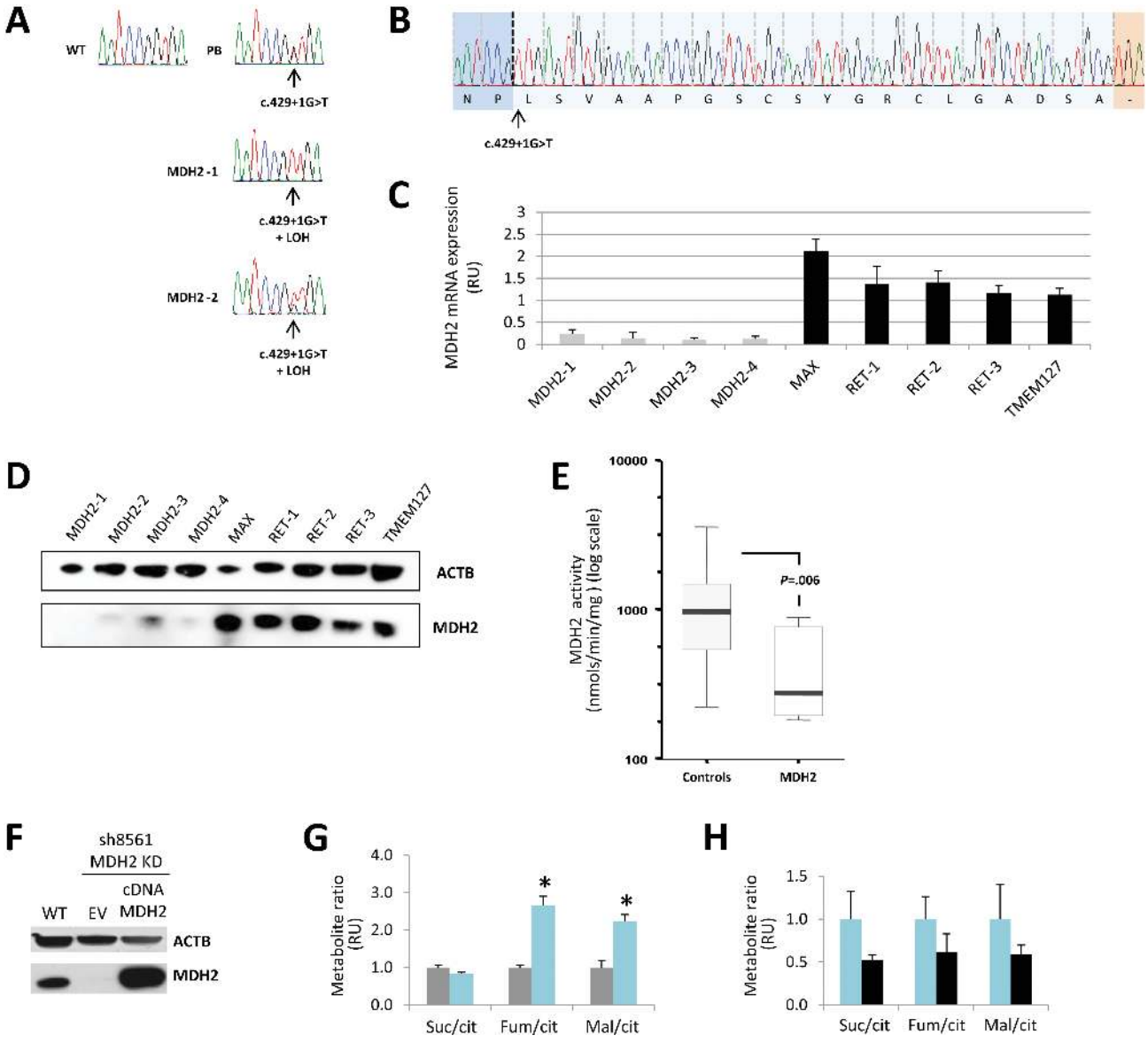

Figure 1. Characterization of *MDH2*-mutated tumors. **A)** *MDH2* mutation in germline DNA from the patient and loss of the wild-type (WT) allele in two tumors of the patient. **B)** Sequence of the aberrant transcript caused by the *MDH2* mutation. **C)** MDH2 mRNA expression in the four *MDH2*-mutated paragangliomas available from the index patient and genetically characterized pheochromocytoma/paraganglioma. Expression level was normalized to β-actin (ACTB) and presented as mean and standard deviation (n ≥ 3). **Error bars** represent standard deviation. **D)** MDH2 western blot of mutated tumors and controls. ACTB was used as a loading control. **E)** Representation of MDH2 activity measured in *MDH2*-mutated and control tumors. The **black line** at the middle of the **box** represents the median. **Whiskers** represent Minimum-Q1, Q3-maximum ranges. MDH2-mutated values from six repeated measurements. *P* value based on a two-sided Mann-Whitney U test. **F)** Western blot of MDH2 KD HeLa cells transfected with a plasmid containing the full cDNA sequence of the human *MDH2* gene (pCMV6-AC-MDH2; Origene), compared with MDH2 KD cells transfected with empty vector (EV) and with untransfected WT HeLa cells. ACTB was used as a loading control. **G)** Metabolite ratios assessed by liquid chromatographic tandem-mass spectrometry in MDH2 KD (**blue bars**) compared with WT (**gray bars**) HeLa cells. The ratios were normalized relative to WT control values and reported as mean and standard deviation (n = 3). A two-sided t test for independent samples was applied to test for differences. *: $P < .05$. **Error bars** represent standard deviations. **H)** Metabolite ratios for MDH2 KD cells transfected with pCMV6-AC-MDH2 (**black bars**) compared with MDH2 KD cells transfected with EV (**blue bars**). The ratios were normalized relative to control (EV) values and reported as mean + SD (n = 3). A two-sided t test for independent samples was applied to test for differences. **Error bars** represent standard deviations. *MDH2* = malate dehydrogenase 2.

effect of a germline *MDH2* mutation identified by whole-exome sequencing. We have also confirmed the absence of MDH2 protein in tumors carrying the variant, as well as the segregation of the c.429+1G>T mutation with the disease, suggesting that *MDH2* behaves as a classic tumor suppressor gene.

The *MDH2*-mutated tumor had not only a global transcriptional profile similar to SDH gene-mutated tumors, but also a CIMP-like signature consistent with Krebs cycle disruption. *Mdh2* function abrogation in *Drosophila* pupae results in a severe energy deficit and accumulation of late-stage Krebs cycle intermediates such as malate, succinate, and fumarate (15). A similar mechanism occurs in *Fh1*-deficient cells that accumulate fumarate and succinate (16). In the present study we have demonstrated that stable silencing of *MDH2* expression in HeLa cells also leads to malate and fumarate accumulation. Like succinate and fumarate, malate inhibits hypoxia inducible factor alpha (HIF-α) prolyl hydroxylation (17,18). Though no malate accumulation was found in the *MDH2*-mutated tumor,

Downloaded from https://academic.oup.com/jnci/article/107/5/djv053/891892 by guest on 25 August 2022

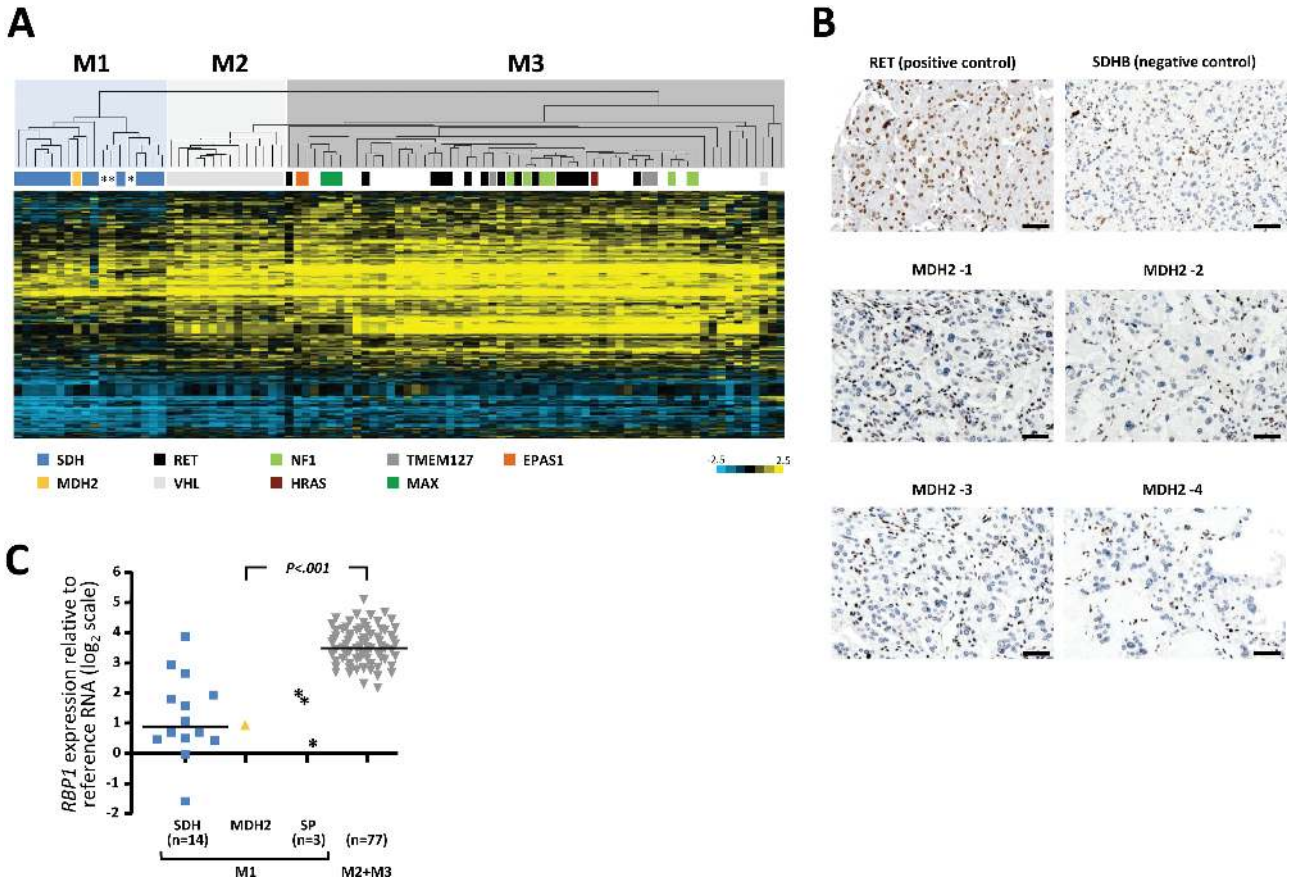

Figure 2. Expression analyses carried out in the *MDH2*-mutated tumors. **A)** Hierarchical clustering of 91 genetically characterized pheochromocytomas/paragangliomas based on expression data for genes hypermethylated and downregulated in SDH/*FH*-mutated pheochromocytomas (5). Three clusters, mimicking those previously obtained using methylation data, were observed and named M1 (CIMP-like), enriched with SDH gene-mutated tumors, M2 with *VHL*-mutated tumors, and M3 with *RET/NF1/MAX/TMEM127*-mutated tumors. Tumors with no color are apparently sporadic cases. **Asterisks** denote three CIMP-like tumors with no identified mutations in the SDH genes, *FH* or *MDH2*. **B)** Immunohistochemical staining of 5-hmC in *MDH2*-, *RET*-, and *SDHB*-mutated tumors. Nuclear 5-hmC was almost undetectable in *MDH2*- and *SDHB*-mutated tumor cells; it was observed only in sustentacular and some stromal cells. The **scale bar** represents 50 μm. **C)** mRNA expression of *RBP1* in the *MDH2*-mutated tumor, SDH gene-mutated tumors, the CIMP-like apparently sporadic tumors clustered in M1 **(A)** and tumors clustered in the M2 and M3 groups **(A)**, defined based on gene expression. *P* value based on a two-sided exact Mann-Whitney U test. The **horizontal black line** represents the median. **Filled squares** and **triangles** represent individual datapoints. *FH* = fumarate hydratase; *MAX* = MYC-associated factor X; *MDH2* = malate dehydrogenase 2; *NF1* = neurofibromin 1; *RBP1* = retinol binding protein 1; *RET* = ret proto-oncogene; SDH = succinate dehydrogenase; *TMEM127* = transmembrane protein 127.

the high fumarate:succinate ratio detected suggests that fumarate accumulation may have been present, which would explain the CIMP-like profile observed. The finding of three SDH gene-, *FH*-, and *MDH2*-negative tumors exhibiting the CIMP-like signature points to the possibility that other, still hidden, molecular alterations in the Krebs cycle account for these cases, and for an unknown proportion of additional patients. The absence of paraganglioma in one of the three c.429+1G>T carriers suggests that the penetrance of mutations in this gene is incomplete, as is the case for *SDHB* mutations (19). Interestingly, none of the seven *FH* mutation carriers described so far with pheochromocytoma/paraganglioma has a family history of the disease (20). Moreover, mutations in the more recently discovered pheochromocytoma/paraganglioma susceptibility genes (*MAX*, *TMEM127*, and *FH*) are present in less than 2% of cases without mutations in known genes (1,13), and in fact none of the 239 Spanish patients screened for mutations was found to be carrier of an *FH* mutation. Finding additional *MDH2* mutation carriers will presumably require genetic screening of large cohorts of patients. Finally, only one truncating mutation (p.E153*) in *MDH2* is recorded in The Catalogue of Somatic Mutations in Cancer (COSMIC; http://cancer.sanger.ac.uk/cancergenome/projects/cosmic/). The mutation was found in a neuroblastoma, a highly metastatic malignancy of the sympathetic nervous system that is genetically related to pheochromocytoma (21) and that also originates primarily in the adrenal gland.

This study is limited by the number of mutation carriers in the pedigree and the incomplete penetrance observed for the *MDH2* alteration. The identification of additional disease-causing mutations in *MDH2* will provide further information about the clinical relevance of this gene. Though we have no explanation for the absence of malate accumulation in the *MDH2*-mutated tumor, we have demonstrated using HeLa cells that *MDH2* abrogation leads to increased levels of malate and the onco-metabolite fumarate.

In summary, whole-exome sequencing has identified a novel tumor suppressor gene, *MDH2*, associated with paraganglioma development. This finding further links the disruption of the Krebs cycle to cancer etiology and highlights that alterations in this major metabolic pathway may explain additional pheochromocytoma/paraganglioma cases.

Funding

This work was supported in part by the Fondo de Investigaciones Sanitarias (grants PI12/00236 and PI11/01359 to AC and MR, respectively), FP7 grant HEALTH-F2-2010–259735

BRIEF COMMUNICATION

Downloaded from https://academic.oup.com/jnci/article/107/5/djv053/891892 by guest on 25 August 2022

(ENS@T-CANCER). SR and GE were supported by the Deutsche Forschungsgemeinschaft EI855/1/1.

Notes

Accession code: A full listing of the exome sequencing results and microarray results has been deposited in the ArrayExpress database (accession code: E-MTAB-2422) and the National Center for Biotechnology Information GEO database (accession number: GSE56573), respectively.

We thank the patient's relatives for their participation in this study. We also thank Centro Nacional de Análisis Genómico (CNAG) personnel, and especially Raul Tonda, for their support in whole-exome sequencing. MCF is a predoctoral fellow of the Severo Ochoa Program, VM and MAR are predoctoral fellows of the "la Caixa"/CNIO international PhD programme, and LIP is a predoctoral fellow of CIBERER. We thank Maria Jesús Artiga and Manuel Morente for their help to obtain tumor samples, collected from Spanish hospitals through the Spanish National Tumor Bank Network (CNIO).

Author contributions: The project was conceived by AC and MR. Samples and clinical information were collected by MCF, MU, MC, SA, and APB. Clinical screening in mutation carriers was performed by RVV and JA. Whole-exome sequencing data analysis and filtering was performed by ICM and AC. mRNA and protein expression analyses were performed by AC, ARM, ICM, AAdC, and VM. Protein activity analysis was performed by LC and JS. Metabolite analysis was performed by SR, MP, and GE. Methylation analysis was performed by SM. Additional experiments were performed by ICM, FS, ME, JFG, GR, AGG, RL, MAR, and LIP. Additional data analysis was performed by AC and ICM. The manuscript was written and revised by AC, ICM, CRA, and MR. All authors approved the final version.

References

1. Dahia PL. Pheochromocytoma and paraganglioma pathogenesis: learning from genetic heterogeneity. *Nat Rev Cancer*. 2014;14(2):108–119.
2. Nagy E, Maquat LE. A rule for termination-codon position within intron-containing genes: when nonsense affects RNA abundance. *Trends Biochem Sci*. 1998;23(6):198–199.
3. Xiao M, Yang H, Xu W, et al. Inhibition of alpha-KG-dependent histone and DNA demethylases by fumarate and succinate that are accumulated in mutations of FH and SDH tumor suppressors. *Genes Dev*. 2012;26(12):1326–1338.
4. Xu W, Yang H, Liu Y, et al. Oncometabolite 2-hydroxyglutarate is a competitive inhibitor of alpha-ketoglutarate-dependent dioxygenases. *Cancer Cell*. 2011;19(1):17–30.
5. Letouze E, Martinelli C, Loriot C, et al. SDH mutations establish a hypermethylator phenotype in paraganglioma. *Cancer Cell*. 2013;23(6):739–752.
6. Chou AP, Chowdhury R, Li S, et al. Identification of retinol binding protein 1 promoter hypermethylation in isocitrate dehydrogenase 1 and 2 mutant gliomas. *J Natl Cancer Inst*. 2012;104(19):1458–1469.
7. Baysal BE, Ferrell RE, Willett-Brozick JE, et al. Mutations in SDHD, a mitochondrial complex II gene, in hereditary paraganglioma. *Science*. 2000;287(5454):848–851.
8. Niemann S, Muller U. Mutations in SDHC cause autosomal dominant paraganglioma, type 3. *Nat Genet*. 2000;26(3):268–270.
9. Astuti D, Latif F, Dallol A, et al. Gene mutations in the succinate dehydrogenase subunit SDHB cause susceptibility to familial pheochromocytoma and to familial paraganglioma. *Am J Hum Genet*. 2001;69(1):49–54.
10. Burnichon N, Briere JJ, Libe R, et al. SDHA is a tumor suppressor gene causing paraganglioma. *Hum Mol Genet*. 2010;19(15):3011–3020.
11. Hao HX, Khalimonchuk O, Schraders M, et al. SDH5, a gene required for flavination of succinate dehydrogenase, is mutated in paraganglioma. *Science*. 2009;325(5944):1139–1142.
12. Tomlinson IP, Alam NA, Rowan AJ, et al. Germline mutations in FH predispose to dominantly inherited uterine fibroids, skin leiomyomata and papillary renal cell cancer. *Nat Genet*. 2002;30(4):406–410.
13. Castro-Vega LJ, Buffet A, De Cubas AA, et al. Germline mutations in FH confer predisposition to malignant pheochromocytomas and paragangliomas. *Hum Mol Genet*. 2014.
14. Gaal J, Burnichon N, Korpershoek E, et al. Isocitrate dehydrogenase mutations are rare in pheochromocytomas and paragangliomas. *J Clin Endocrinol Metab*. 2010;95(3):1274–1278.
15. Wang L, Lam G, Thummel CS. Med24 and Mdh2 are required for Drosophila larval salivary gland cell death. *Dev Dyn*. 2010;239(3):954–964.
16. Frezza C, Zheng L, Folger O, et al. Haem oxygenase is synthetically lethal with the tumour suppressor fumarate hydratase. *Nature*. 2011;477(7363):225–228.
17. Philip B, Ito K, Moreno-Sanchez R, Ralph SJ. HIF expression and the role of hypoxic microenvironments within primary tumours as protective sites driving cancer stem cell renewal and metastatic progression. *Carcinogenesis*. 2013;34(8):1699–1707.
18. Pan Y, Mansfield KD, Bertozzi CC, et al. Multiple factors affecting cellular redox status and energy metabolism modulate hypoxia-inducible factor prolyl hydroxylase activity in vivo and in vitro. *Mol Cell Biol*. 2007;27(3):912–925.
19. Schiavi F, Milne RL, Anda E, et al. Are we overestimating the penetrance of mutations in SDHB? *Hum Mutat*. 2010;31(6):761–762.
20. Clark GR, Sciacovelli M, Gaude E, et al. Germline FH mutations presenting with pheochromocytoma. *J Clin Endocrinol Metab*. 2014;99(10):E2046–E2050.
21. Schimke RN, Collins DL, Stolle CA. Paraganglioma, neuroblastoma, and a SDHB mutation: Resolution of a 30-year-old mystery. *Am J Med Genet A*. 2010;152A(6):1531–1535.

Downloaded from https://academic.oup.com/jnci/article/107/5/djv053/891892 by guest on 25 August 2022

BRIEF COMMUNICATION